Model. Simul. Mater. Sci. Eng., in press (2013)

# Conditional Convergence in 2-Dimensional Dislocation Dynamics

**William P. Kuykendall‡ and Wei Cai**

Department of Mechanical Engineering, Stanford University, CA 94305-4040

**Abstract.** For 2-dimensional dislocation dynamics (DD) simulations under periodic boundary conditions (PBC) in both directions, the summation of the periodic image stress fields is found to be conditionally convergent. For example, different stress fields are obtained depending on whether the summation in the $x$-direction is performed before or after the summation in the $y$-direction. This problem arises because the stress field of a 1D periodic array of dislocations does not necessarily go to zero far away from the dislocation array. The spurious stress fields caused by conditional convergence in the 2D sum are shown to consist of only a linear term and a constant term with no higher order terms. Absolute convergence, and hence self-consistency, is restored by subtracting the spurious stress fields, whose expressions have been derived in both isotropic and anisotropic elasticity.

‡ Corresponding Author: wpkuyken@stanford.edu

## 1. Introduction

Two dimensional dislocation dynamics (DD) simulations have been utilized for more than two decades. While the 2D model is a simplification of the 3D dislocation microstructure in real crystals, it has been successfully applied to account for many aspects of dislocation physics. Most of the 2D DD simulations have focused on edge dislocations [1, 2, 3, 4, 5, 6, 7, 8, 9, 10, 11, 12, 13, 14], but screw dislocations have been simulated as well [2]. Both linear and non-linear mobility laws have been devised and both glide [1, 3, 5, 8, 9, 11, 12, 13, 14] and climb [2, 3, 7, 8] are allowed. Dislocations on a single slip system [1, 5, 6, 9, 10, 11, 13] or multiple slip systems [3, 7, 8, 10, 12, 14] can be modelled. Dislocation sources [1, 2, 3, 5, 9, 10, 11, 12, 13, 14] and obstacles (inclusions) [1, 5, 9, 14] have been introduced. The loading condition can be either constant strain rate [9, 12, 14], constant stress (creep) [1, 11], or cyclic [3, 11]. Periodic boundary conditions in one [5, 10] or both directions [3, 7, 8, 9, 12] are often used for bulk simulations. For DD simulations in a finite sample, image stress solvers have been developed to allow dislocations to interact with the sample surface, as well as with a crack in fracture simulations [4, 10, 13]. Periodic boundary conditions (PBC) are usually applied to DD simulations of bulk crystals. In 2D DD, PBC along one direction can be easily applied because the stress field of an infinite linear array of singular dislocations is known analytically. When PBC are applied in both directions, the stress field of a 2-dimensional array of dislocations is needed. Because only the summation over one direction can be performed analytically, the summation over the other direction has to be performed numerically. For self-consistency, the final result should be independent of which direction (i.e. $x$ or $y$) the summation is performed analytically (or numerically). Unfortunately, due to the long-range nature of dislocation stress fields, a naïve approach will lead to different results depending on the order of the summation, which is the signature of conditional convergence. Therefore, the stress obtained from the numerical sum contains the true solution plus a "spurious" stress field. We solve this problem by subtracting the spurious stress fields so that absolute convergence is restored. The spurious stress fields are shown to contain a linear term and a constant term and their analytic expressions are derived in both isotropic and anisotropic elasticity. From the analytic expressions, we found that when all dislocations are edge dislocations gliding along parallel (either $x$ or $y$) planes, then the conditional convergence problem does not introduce a non-zero glide force on the dislocations. However, the conditional convergence problem will introduce non-zero error in the force when dislocations on multiple systems are considered, or when climb is allowed, or if the Burgers vector contains non-zero screw component. The rest of this paper is organized as follows. In Section 2, the degrees of freedom and types of boundary conditions in 2D DD are introduced. In Section 3, the singular stress fields in 2D are discussed in more detail, and the (previously known [16]) analytical expressions for 1D periodic array of dislocations are summarized. In Section 4, the problem of conditional convergence in 2D doubly periodic simulations is introduced and solved. The spurious linear stress field is shown to depend on the net Burgers vector (i.e. monopole moment) in the simulation cell. The spurious constant

stress field is shown to depend on the net dipole moment. The analytic expressions of these spurious terms are derived in isotropic elasticity. In Section 5, the solution of the conditional convergence problem is generalized to anisotropic elasticity.

## 2. Model Description

We implemented a 2D DD simulation program in `Matlab`. The dislocations are assumed to be straight and infinitely long in the $z$-direction and are modelled as point objects moving in the $x$-$y$ plane. Each dislocation $q$ is specified by three main pieces of information: position $\mathbf{r}^{(q)} = (x^{(q)}, y^{(q)})$, Burgers vector $\mathbf{b}^{(q)} = (b_x^{(q)}, b_y^{(q)}, b_z^{(q)})$, and glide plane normal $\mathbf{n}^{(q)} = (n_x^{(q)}, n_y^{(q)})$. Note that the Burgers vector is a 3D vector so that the character of the dislocations can be edge, screw, or mixed.

The dislocations reside in a homogenous linear elastic medium. Our current implementation assumes an isotropic elastic medium. DD simulations in a 2D anisotropic elastic medium exist [17], to which our solution to the conditional convergence problem can be extended. For simplicity, we consider only four types of boundary conditions: (1) infinite in both $x$ and $y$ (specified dislocations are the only ones present in a medium of infinite extent); (2) periodic in $x$ and infinite in $y$; (3) periodic in $y$ and infinite in $x$; and (4) periodic in both $x$ and $y$. In case (4) (i.e. doubly periodic), the simulation cell is a supercell with a rectangular shape.

In case (1), the stress field at each dislocation is obtained by summing the contribution from all other dislocations in the simulation cell. The singular stress expressions due to each dislocation $q$ are given in Section 3.1. In cases (2) and (3), each dislocation $q$ in the simulation cell corresponds to a linear array of dislocations. Fortunately, the stress field of a linear array of singular dislocations is known analytically both in isotropic [16] and anisotropic media [17]. In case (4), each dislocation $q$ in the simulation cell corresponds to 2D periodic array of dislocations, as shown in figure 1. To obtain its stress contribution, only the summation over one direction ($x$ or $y$) can be summed analytically and the summation over the other direction ($y$ or $x$) must be performed numerically as a finite sum involving a truncation. The number of image cells in the direction of numerical summation is an option that can be adjusted, though the results tend to converge quite quickly (usually within about three image cells in both positive and negative directions). Obviously, there is a choice of which direction the sum is performed analytically (and numerically for the other direction) and the final result should be independent of this choice. However, care must be taken to address the conditional convergence problem as discussed in Section 4.

## 3. Stresses

The stresses resulting from one infinitely long straight dislocation are well known in both isotropic and anisotropic media [16]. However, to understand how the conditional convergence term develops, it is useful to have the stress fields of a single dislocation and a

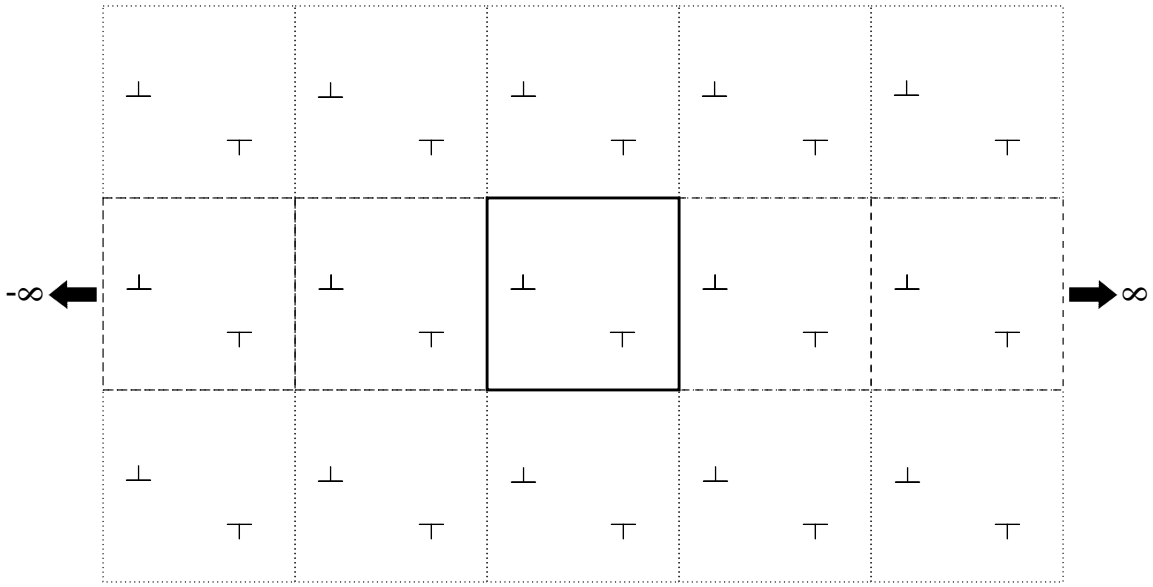


**Figure 1.** A DD simulation cell with doubly periodic boundary conditions. The primary cell is the solid box. The analytical summation is in the $x$-direction (dashed lines). The numerical summation is in the $y$-direction (dotted lines).

1D periodic array of dislocations available. This is because the conditional convergence term arises from the fact that certain stress components do not necessarily go to zero far from a 1D array. Instead, these components go to a constant fairly quickly.

### *3.1. Single Dislocation*

The stress field of an infinitely long straight dislocation in an isotropic medium is reproduced below [16]. For an edge dislocation along the $z$-axis, the non-zero stress components are,

$$\sigma_{xy}(x,y) = \frac{\mu}{2\pi(1-\nu)}\left[\frac{b_x\,x}{x^2+y^2}\left(1-\frac{2y^2}{x^2+y^2}\right)-\frac{b_y\,y}{x^2+y^2}\left(1-\frac{2x^2}{x^2+y^2}\right)\right], \quad (1)$$

$$\sigma_{yy}(x,y) = \frac{\mu}{2\pi(1-\nu)}\left[\frac{b_x\,y}{x^2+y^2}\left(1-\frac{2y^2}{x^2+y^2}\right)+\frac{b_y\,x}{x^2+y^2}\left(1+\frac{2y^2}{x^2+y^2}\right)\right], \quad (2)$$

$$\sigma_{xx}(x,y) = \frac{-\mu}{2\pi(1-\nu)}\left[\frac{b_x\,y}{x^2+y^2}\left(1+\frac{2x^2}{x^2+y^2}\right)+\frac{b_y\,x}{x^2+y^2}\left(1-\frac{2x^2}{x^2+y^2}\right)\right]. \quad (3)$$

where $\mu$ and $\nu$ are the shear modulus and Poisson's ratio, respectively. For a screw dislocation along the $z$-axis, the non-zero stress fields are

$$\sigma_{xz}(x,y) = \frac{-\mu b_z}{2\pi}\frac{y}{x^2+y^2}, \quad (4)$$

$$\sigma_{yz}(x,y) = \frac{\mu b_z}{2\pi}\frac{x}{x^2+y^2}. \quad (5)$$

### *3.2. 1D Periodic Array of Dislocations*

For a dislocation array arranged along the $x$ direction with periodicity $\mathcal{L}_x$ and Burgers vector $\mathbf{b} = (b_x, b_y, b_z)$, the stress field can be obtained from an infinite summation,

$$\boldsymbol{\sigma}^{\text{xPBC}}(x,y) = \sum_{m=-\infty}^{+\infty} \boldsymbol{\sigma}(x - m\mathcal{L}_x, y) \tag{6}$$

where $\boldsymbol{\sigma}(x,y)$ is the stress field of a single dislocation, as given in Eqs.(1)-(5). This summation can be performed analytically and the results are given below.

$$\sigma_{xy}^{\text{xPBC}} = \frac{\mu b_x s_X}{2(1-\nu)\mathcal{L}_x}\left[\frac{(C_Y - c_X) - 2\pi Y S_Y}{(C_Y - c_X)^2}\right] - \frac{\mu b_y \pi Y}{(1-\nu)\mathcal{L}_x}\left[\frac{C_Y c_X - 1}{(C_Y - c_X)^2}\right], \tag{7}$$

$$\sigma_{yy}^{\text{xPBC}} = \frac{-\mu b_x \pi Y}{(1-\nu)\mathcal{L}_x}\left[\frac{C_Y c_X - 1}{(C_Y - c_X)^2}\right] + \frac{\mu b_y s_X}{2(1-\nu)\mathcal{L}_x}\left[\frac{2\pi Y S_Y + C_Y - c_X}{(C_Y - c_X)^2}\right], \tag{8}$$

$$\begin{aligned}\sigma_{xx}^{\text{xPBC}} = {} & \frac{\mu b_x}{(1-\nu)\mathcal{L}_x}\left[\frac{\pi Y(C_Y c_X - 1) - S_Y(C_Y - c_X)}{(C_\phi - c_X)^2}\right] \\ & + \frac{\mu b_y s_X}{2(1-\nu)\mathcal{L}_x}\left[\frac{C_Y - c_X - 2\pi Y S_Y}{(C_\phi - c_X)^2}\right],\end{aligned} \tag{9}$$

$$\sigma_{xz}^{\text{xPBC}} = \frac{-\mu b_z}{2\mathcal{L}_x}\left[\frac{S_Y}{C_Y - c_X}\right], \tag{10}$$

$$\sigma_{yz}^{\text{xPBC}} = \frac{\mu b_z}{2\mathcal{L}_x}\left[\frac{s_X}{C_Y - c_X}\right], \tag{11}$$

where

$$X = \frac{x}{\mathcal{L}_x} \tag{12}$$

$$Y = \frac{y}{\mathcal{L}_x} \tag{13}$$

$$s_X = \sin 2\pi X \tag{14}$$

$$c_X = \cos 2\pi X \tag{15}$$

$$S_Y = \sinh 2\pi Y \tag{16}$$

$$C_Y = \cosh 2\pi Y. \tag{17}$$

Similarly, for a dislocation array along the $y$ direction with periodicity $\mathcal{L}_y$, the stress fields can be obtained from an infinite summation,

$$\boldsymbol{\sigma}^{\text{yPBC}}(x,y) = \sum_{n=-\infty}^{+\infty} \boldsymbol{\sigma}(x, y - n\mathcal{L}_y) \tag{18}$$

where $\boldsymbol{\sigma}(x,y)$ is the stress field of a single dislocation, as given in Eqs.(1)-(5). This summation has been derived analytically before [16] (pp 733-734), and the results are reproduced below.

$$\sigma_{xy}^{\text{yPBC}} = \frac{\mu b_x \pi X}{(1-\nu)\mathcal{L}_y}\left[\frac{C_X c_Y - 1}{(C_X - c_Y)^2}\right] + \frac{\mu b_y s_Y}{2(1-\nu)\mathcal{L}_y}\left[\frac{2\pi X S_X - C_X + c_Y}{(C_X - c_Y)^2}\right], \tag{19}$$

$$\sigma_{yy}^{\text{yPBC}} = \frac{\mu b_x s_Y}{2(1-\nu)\mathcal{L}_y}\left[\frac{2\pi X S_X - C_X + c_Y}{(C_X - c_Y)^2}\right] - \frac{\mu b_y}{(1-\nu)\mathcal{L}_y}\left[\frac{\pi X(C_X c_Y - 1) - S_X(C_X - c_Y)}{(C_X - c_Y)^2}\right], \tag{20}$$

$$\sigma_{xx}^{\text{yPBC}} = \frac{-\mu b_x s_Y}{2(1-\nu)\mathcal{L}_y}\left[\frac{2\pi X S_X + C_X - c_Y}{(C_X - c_Y)^2}\right] + \frac{\mu b_y \pi X}{(1-\nu)\mathcal{L}_y}\left[\frac{C_X c_Y - 1}{(C_X - c_Y)^2}\right], \tag{21}$$

$$\sigma_{xz}^{\text{yPBC}} = \frac{-\mu b_z}{2\mathcal{L}_y}\left[\frac{s_Y}{C_X - c_Y}\right], \tag{22}$$

$$\sigma_{yz}^{\text{yPBC}} = \frac{\mu b_z}{2\mathcal{L}_y}\left[\frac{S_X}{C_X - c_Y}\right], \tag{23}$$

where

$$X = \frac{x}{\mathcal{L}_y} \tag{24}$$

$$Y = \frac{y}{\mathcal{L}_y} \tag{25}$$

$$s_Y = \sin 2\pi Y \tag{26}$$

$$c_Y = \cos 2\pi Y \tag{27}$$

$$S_X = \sinh 2\pi X \tag{28}$$

$$C_X = \cosh 2\pi X. \tag{29}$$

## 4. Conditional Convergence of Doubly Periodic Boundary Conditions

### *4.1. Problem Statement*

When the simulation cell containing $N$ dislocations is under PBC in both $x$ and $y$ directions, the stress field at a given point $\mathbf{r}^P = (x^P, y^P)$ can be nominally written as,

$$\boldsymbol{\sigma}^{\text{xyPBC}}(x^P, y^P) = \sum_{q=1}^{N}\sum_{m=-\infty}^{+\infty}\sum_{n=-\infty}^{+\infty}\boldsymbol{\sigma}^{(q)}(x^P - x^{(q)} - m\mathcal{L}_x, y^P - y^{(q)} - n\mathcal{L}_y) \tag{30}$$

where $\boldsymbol{\sigma}^{(q)}(x, y)$ is the stress field of a dislocation with Burgers vector $\mathbf{b}^{(q)}$ at the origin, as given in Eqs.(1)-(5). § One of the two infinite summations can be performed analytically. Without loss of generality, let us assume that the summation along the $x$-direction is performed analytically. Hence,

$$\boldsymbol{\sigma}^{\text{xyPBC}}(x^P, y^P) = \sum_{q=1}^{N}\sum_{n=-\infty}^{+\infty}\boldsymbol{\sigma}^{\text{xPBC}(q)}(x^P - x^{(q)}, y^P - y^{(q)} - n\mathcal{L}_y) \tag{31}$$

§ In DD simulations, point $\mathbf{r}^P$ is often the location of one of the dislocations. When singular stress expressions are used, the stress field due to the dislocation at point $\mathbf{r}^P$ must be explicitly excluded, in order to avoid numerical overflow. In contrast, no dislocation needs to be excluded if non-singular stress expressions [15] are used.

This summation has to be performed numerically, so that in practice a truncation scheme is needed. There are several truncation schemes to choose from. First, we can include all periodic image dislocations (along $y$-axis) that are within a cut-off distance, $N_c\mathcal{L}_y$, of the field point $y^P$, i.e.

$$\boldsymbol{\sigma}^{\text{xyPBC}}(x^P, y^P) \stackrel{?}{=} \lim_{N_c\to\infty} \sum_{q=1}^{N} \sum_{\substack{n \\ |y^P - y^{(q)} - n\mathcal{L}_y| \,\le\, N_c\mathcal{L}_y}} \boldsymbol{\sigma}^{\text{xPBC}(q)}(x^P - x^{(q)}, y^P - y^{(q)} - n\mathcal{L}_y) \quad (32)$$

Note that which periodic images are included in the sum depends on both the field point $y^P$ and the dislocation $y^{(q)}$. The problem with this approach is that the resulting stress field can exhibit discontinuities (as $y^P$ changes) when $\lim_{y\to\infty} \boldsymbol{\sigma}^{\text{xPBC}}(x, y) \neq 0$, which has been demonstrated numerically (see figure 3(d)). Therefore, we will adopt the second truncation scheme described below.

In the second truncation scheme, the same set of periodic images are included for all dislocations regardless of the field point, i.e.

$$\boldsymbol{\sigma}^{\text{xyPBC}}(x^P, y^P) \stackrel{?}{=} \lim_{N_c\to\infty} \sum_{n=-N_c}^{N_c} \sum_{q=1}^{N} \boldsymbol{\sigma}^{\text{xPBC}(q)}(x^P - x^{(q)}, y^P - y^{(q)} - n\mathcal{L}_y) \quad (33)$$

Recall that in arriving at Eq. (33) we have let the summation in $x$-direction be performed analytically and the summation in $y$-direction be performed numerically. Alternatively, we can reverse this choice to arrive at the following approximation,

$$\boldsymbol{\sigma}^{\text{xyPBC}}(x^P, y^P) \stackrel{?}{=} \lim_{N_c\to\infty} \sum_{m=-N_c}^{N_c} \sum_{q=1}^{N} \boldsymbol{\sigma}^{\text{yPBC}(q)}(x^P - x^{(q)} - m\mathcal{L}_x, y^P - y^{(q)}) \quad (34)$$

For self-consistency, we expect Eqs. (33) and (34) to give identical results. However, it can be easily demonstrated numerically that this is not the case (hence the question marks on the equal signs). This is the problem of conditional convergence, which we will address in the rest of this section.

### *4.2. Nature of Conditional Convergence*

The inconsistency between Eqs. (33) and (34) can be viewed in a broader context described below. Define

$$\boldsymbol{\sigma}^{\text{cell}}(x^P, y^P; m, n) \equiv \sum_{q=1}^{N} \boldsymbol{\sigma}^{(q)}(x^P - x^{(q)} - m\mathcal{L}_x, y^P - y^{(q)} - n\mathcal{L}_y) \quad (35)$$

as the stress at point $\mathbf{r}^P$ due to all dislocations contained in an image cell $(m, n)$. Then Eq. (30) becomes

$$\boldsymbol{\sigma}^{\text{xyPBC}}(x^P, y^P) \stackrel{?}{=} \sum_{m,n=-\infty}^{+\infty} \boldsymbol{\sigma}^{\text{cell}}(x^P, y^P; m, n) \quad (36)$$

In practice, a truncation scheme must be introduced to perform this summation numerically. For example, we can include contributions from all image cells within a rectangle and increase the size of the rectangle until the value converges to desirable accuracy, as illustrated in figure 2(a). Other possible truncation schemes are illustrated in figure 2(b), (c), and (d). Eq. (33) corresponds to the case where the boundary of $m$ goes to infinity *before* the boundary of $n$ goes to infinity. This can be visualized as adopting rectangular truncation domains in the limit of its aspect ratio ($x$-dimension over $y$-dimension) going to infinity. On the other hand, Eq. (34) corresponds to adopting rectangular truncation domains in the limit of its aspect ratio going to zero. The inconsistency between Eqs. (33) and (34) means the numerical sum depends on order of summation.

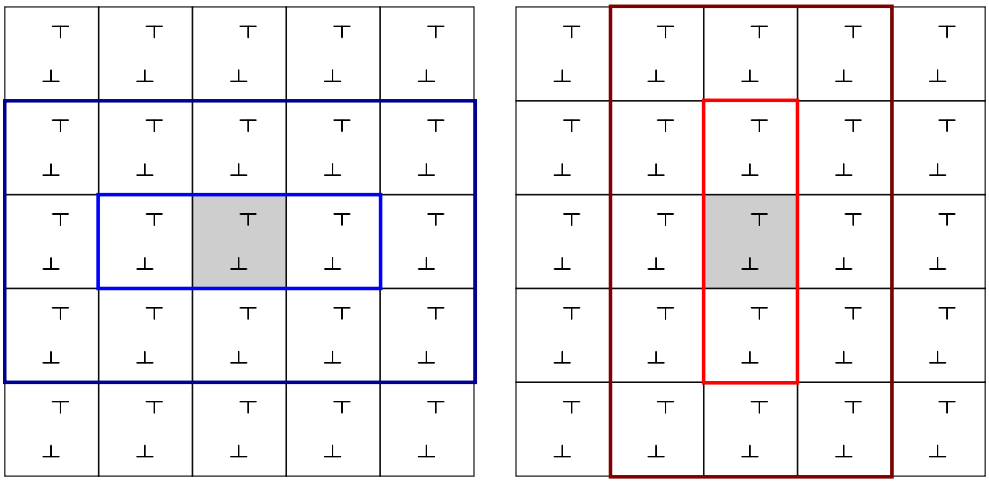

(a) Horizontal Rectangle

(b) Vertical Rectangle

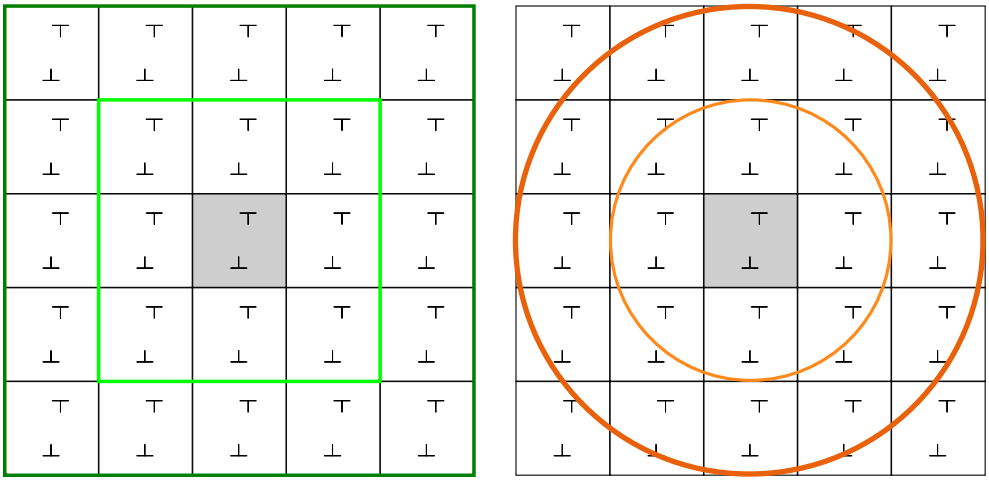

(c) Square

(d) Circle

**Figure 2.** Different truncation schemes. The shaded cell is the primary cell. The lighter and darker shapes show smaller and larger cut-off regions included in the sum, respectively.

A summation series is *conditionally convergent* when, as the number of terms goes to infinity, the sum approaches some finite value, but this value depends on the order of the terms in the summation [18]. In the 2-dimensional summation considered here, this dependence on the order of summation is equivalent to the dependence on the shape of the truncation domain.

In contrast, a summation series that is independent of the order of summation is called *absolutely convergent*. An absolutely convergent sum is one that the sum of the absolute values of every term is also convergent, while for a conditionally convergent sum the sum of the absolute values of every term is divergent (Riemann series theorem [19]). This allows us to test whether a summation series suffers from conditional convergence.

The stress field of a dislocation scales as $1/r$, where $r \equiv \sqrt{x^2+y^2}$ is the distance between the dislocation and the field point. Therefore, if the total Burgers vector in the simulation cell,

$$\mathbf{b}^{\text{tot}} \equiv \sum_{q=1}^{N} \mathbf{b}^{(q)} \tag{37}$$

is non-zero, then for large enough $m$ and $n$, we expect

$$\boldsymbol{\sigma}^{\text{cell}}(x^P, y^P; m, n) \propto \frac{1}{R} \tag{38}$$

where $R \equiv \sqrt{(m\mathcal{L}_x)^2 + (n\mathcal{L}_y)^2}$. This allows us to estimate the far-field contribution to the sum in Eq. (36) when the absolute values are summed.

$$\sum_{m,n=-\infty}^{+\infty} |\boldsymbol{\sigma}^{\text{cell}}(x^P, y^P; m, n)| \sim \sum_{m,n=-\infty}^{+\infty} \frac{1}{R} \sim \int_c^{\infty} \frac{1}{R}\, 2\pi R \,\mathrm{d}R \to \infty \tag{39}$$

where $c$ is a constant that is sufficiently large. This means that the summation in Eq. (36) is conditionally convergent.

However, the summation becomes absolutely convergent if we sum the second derivatives of the stress field, instead of the stress field itself [20]. This is because the field decays to zero faster every time a spatial derivative is taken.

$$\partial_u \boldsymbol{\sigma}^{\text{cell}}(x^P, y^P; m, n) \propto \frac{1}{R^2} \tag{40}$$

$$\partial_u \partial_v \boldsymbol{\sigma}^{\text{cell}}(x^P, y^P; m, n) \propto \frac{1}{R^3} \tag{41}$$

where $\partial_u \equiv \partial/\partial x_u^P$, $u, v = 1$ or 2, $x_1^P = x^P$, $x_2^P = y^P$. Hence

$$\sum_{m,n=-\infty}^{+\infty} |\partial_u \partial_v \boldsymbol{\sigma}^{\text{cell}}(x^P, y^P; m, n)| \sim \sum_{m,n=-\infty}^{+\infty} \frac{1}{R^3} \sim \int_c^{\infty} \frac{1}{R^3}\, 2\pi R \,\mathrm{d}R \to (\text{finite}) \tag{42}$$

This means that the second derivatives of the stress field under doubly periodic boundary conditions are absolutely convergent, i.e. the following summation does not depend on the truncation schemes,

$$\partial_u \partial_v \boldsymbol{\sigma}^{\text{xyPBC}}(x^P, y^P) = \sum_{m,n=-\infty}^{+\infty} \partial_u \partial_v \boldsymbol{\sigma}^{\text{cell}}(x^P, y^P; m, n) \tag{43}$$

Integrating both sides two times, we find that the error in Eq. (36) contains at most a linear term and a constant term, which, if subtracted, restores the correct solution [20], i.e.

$$\boldsymbol{\sigma}^{\mathrm{xyPBC}}(x^P, y^P) = \sum_{m,n=-\infty}^{+\infty} \boldsymbol{\sigma}^{\mathrm{cell}}(x^P, y^P; m, n) - \mathbf{B}\cdot\mathbf{r}^P - \mathbf{C} \tag{44}$$

where the coefficients $\mathbf{B}$ and $\mathbf{C}$ depends on the truncation scheme employed in the summation. We will call these extra terms "spurious terms" in the following discussions. For the specific truncation schemes employed in Eqs. (33) and (34), we have,

$$\boldsymbol{\sigma}^{\mathrm{xyPBC}}(x^P, y^P) = \lim_{N_c\to\infty} \sum_{n=-N_c}^{N_c} \sum_{q=1}^{N} \boldsymbol{\sigma}^{\mathrm{xPBC}(q)}(x^P - x^{(q)}, y^P - y^{(q)} - n\mathcal{L}_y) - \mathbf{B}^{\mathrm{xanl}}\, y - \mathbf{C}^{\mathrm{xanl}} \tag{45}$$

and

$$\boldsymbol{\sigma}^{\mathrm{xyPBC}}(x^P, y^P) = \lim_{N_c\to\infty} \sum_{m=-N_c}^{N_c} \sum_{q=1}^{N} \boldsymbol{\sigma}^{\mathrm{yPBC}(q)}(x^P - x^{(q)} - m\mathcal{L}_x, y^P - y^{(q)}) - \mathbf{B}^{\mathrm{yanl}}\, x - \mathbf{C}^{\mathrm{yanl}} \tag{46}$$

where "xanl" ("yanl") indicates the summation in $x$ ($y$) direction is performed analytically. Because when the analytic sum is performed along $x$ the resulting field must be periodic along $x$, the linear term in Eq. (45) can only be proportional to $y$. For the same reason, the linear term in Eq. (46) can only be proportional to $x$. Cai et al. [20] developed a method in which the coefficients $\mathbf{B}$ and $\mathbf{C}$ can be computed numerically by introducing "ghost" dislocations at cell boundaries. While this may be necessary for 3-dimensional sums of dislocation fields, in 2-dimensional sums these coefficients can be found analytically, as shown below.

The conditional convergence problem encountered here is quite similar to the Madelung summation problem for electrostatic interactions in ionic crystals. The latter is usually solved by the Ewald method [21], which makes use of the Fourier transform. The analytical solution discussed below is consistent with the Fourier method developed by Boerma [22, 23].

### *4.3. Solution*

Due to symmetries, many components of the tensorial coefficients $\mathbf{B}$ and $\mathbf{C}$ vanish, which may explain why this conditional convergence problem was not well appreciated previously. For example, if the simulation cell contains only edge dislocations with Burgers vector $b_x$, the symmetries of the $\sigma_{xy}$ and $\sigma_{yy}$ fields in isotropic elasticity ensures that the spurious terms vanish. The $\sigma_{xx}$ field, however, contains the spurious terms when the summation is performed analytically in the $x$-direction. Similarly, the spurious terms arise for the $\sigma_{yy}$ field of edge dislocations with Burgers vector $b_y$ and analytical sum in the $y$-direction. The spurious term always arises for the $\sigma_{xz}$ field of screw dislocations when the analytical sum is in the $x$-direction, and for the $\sigma_{yz}$ field when the analytical sum is in the $y$-direction. In

anisotropic elasticity, more components of the spurious stress field are non-zero, while certain components remain zero (see Section 5).

When the analytic sum is in the $x$ direction, the non-zero coefficients of the spurious terms in isotropic elasticity are the following.

$$B_{xx}^{\text{xanl}} = -\frac{2\mu}{(1-\nu)\mathcal{L}_x\mathcal{L}_y}\sum_{q=1}^{N} b_x^{(q)} \tag{47}$$

$$C_{xx}^{\text{xanl}} = \frac{2\mu}{(1-\nu)\mathcal{L}_x\mathcal{L}_y}\sum_{q=1}^{N} b_x^{(q)} y^{(q)} \tag{48}$$

$$B_{xz}^{\text{xanl}} = -\frac{\mu}{\mathcal{L}_x\mathcal{L}_y}\sum_{q=1}^{N} b_z^{(q)} \tag{49}$$

$$C_{xz}^{\text{xanl}} = \frac{\mu}{\mathcal{L}_x\mathcal{L}_y}\sum_{q=1}^{N} b_z^{(q)} y^{(q)} \tag{50}$$

Note that the coefficient $\mathbf{B}$ of the linear spurious field is proportional to the total Burgers vector $\mathbf{b}^{\text{tot}}$ of the simulation cell, while the constant spurious field $\mathbf{C}$ is proportional to the total dipole moment. The similarity between the expressions in $\mathbf{B}$ and $\mathbf{C}$ is also notable.

When the analytic sum is in the $y$ direction, the non-zero coefficients of the spurious terms are the following.

$$B_{yy}^{\text{yanl}} = \frac{2\mu}{(1-\nu)\mathcal{L}_x\mathcal{L}_y}\sum_{q=1}^{N} b_y^{(q)} \tag{51}$$

$$C_{yy}^{\text{yanl}} = -\frac{2\mu}{(1-\nu)\mathcal{L}_x\mathcal{L}_y}\sum_{q=1}^{N} b_y^{(q)} x^{(q)} \tag{52}$$

$$B_{yz}^{\text{yanl}} = \frac{\mu}{\mathcal{L}_x\mathcal{L}_y}\sum_{q=1}^{N} b_z^{(q)} \tag{53}$$

$$C_{yz}^{\text{yanl}} = -\frac{\mu}{\mathcal{L}_x\mathcal{L}_y}\sum_{q=1}^{N} b_z^{(q)} x^{(q)} \tag{54}$$

The expressions corresponding to Eqs. (47)-(54) in anisotropic elasticity are derived in Section 5.

In 2D DD simulations, the total Burgers vector (i.e. monopole moment) is often constrained to be zero, in which case the linear spurious term vanishes. However, the total dipole moment is usually nonzero in DD simulations, allowing for a spurious constant stress field to exist. When the analytic sum is in the $x$-direction, the spurious term arises in the $\sigma_{xx}$ field of edge dislocation with Burgers vector $b_x$. This spurious stress field does not produce a glide force on the dislocations if all Burgers vectors are along the $x$-axis, but will cause spurious forces if edge dislocations on several glide planes exist or if climb is allowed. A 2D simulation cell containing screw dislocations will almost always contain the spurious stress

field under doubly periodic boundary conditions.

It may be argued that a simulation cell containing a non-zero total Burgers vector is incompatible with PBC in both directions. For example, it is impossible to create such a configuration in atomistic simulations. However, it is technically possible to apply PBC in both directions for DD simulations, even when the total Burgers vector is non-zero. Such simulations may potentially reveal the effect of geometrically necessary dislocations on dislocation pattern formation and strain hardening. Therefore, we do not exclude this possibility from our discussion.

### *4.4. Proof*

In the following, we prove Eqs. (47)-(54) in three steps. First, we show that for a 2D DD simulation cell containing zero total Burgers vector $\mathbf{b}^{\text{tot}}$, the coefficients $\mathbf{B}$ for the linear spurious field vanishes, and the constant spurious field $\mathbf{C}$ is proportional to the dipole moment. Second, we show that $\mathbf{C}$ is linked to the far field stress of a periodic 1D array of dislocations using a thought experiment. Third, we use a similar thought experiment to derive the coefficients $\mathbf{B}$.

*4.4.1.* $\mathbf{C}$ *is proportional to dipole moment* The stress field of a dislocation dipole scales as $1/r^2$, where $r \equiv \sqrt{x^2 + y^2}$ is the distance between the dislocation dipole and the field point. Therefore, if the total Burgers vector $\mathbf{b}^{\text{tot}}$ for the simulation cell vanishes, then for large enough $m$ and $n$, we expect

$$\boldsymbol{\sigma}^{\text{cell}}(x^P, y^P; m, n) \propto \frac{1}{R^2} \tag{55}$$

where $R \equiv \sqrt{(m\mathcal{L}_x)^2 + (n\mathcal{L}_y)^2}$. Following the same line of argument as in Eqs. (39)-(44), we can show that the first derivative of the stress field summation is absolutely convergent. Hence the error in Eq. (36) contains at most a constant term, which, if subtracted, restores the correct solution [20], i.e.

$$\boldsymbol{\sigma}^{\text{xyPBC}}(x^P, y^P) = \sum_{m,n=-\infty}^{+\infty} \boldsymbol{\sigma}^{\text{cell}}(x^P, y^P; m, n) - \mathbf{C} \tag{56}$$

This means that $\mathbf{B} = 0$ when $\mathbf{b}^{\text{tot}} = 0$. Similarly, we can show (by linear superposition) that if both the total Burgers vector and the dipole moment vanishes in the simulation cell (i.e. only quadrupole and higher moments exists), then both $\mathbf{B} = 0$ and $\mathbf{C} = 0$ (i.e. the stress field summation is absolutely convergent).

Now consider two simulation cells with different dislocation arrangements but with $\mathbf{b}^{\text{tot}} = 0$, identical cell sizes, as well as the same summation scheme (e.g. analytic in $x$ and numerical in $y$). Given that $\mathbf{C} = 0$ when the dipole moment vanishes, if the two simulation cells have the same dipole moments, then they must also have identical values for $\mathbf{C}$ (which can be shown by subtracting the stress field of the two cells). This means that $\mathbf{C}$ is only a function of the dipole moment, and independent of the other moments of the dislocation

distribution. Furthermore, **C** must be proportional to the dipole moment, because if we double the Burgers vector of every dislocation in the cell, both the dipole moment and **C** must be doubled. By similar arguments, we can show that **B** is proportional to $\mathbf{b}^{\text{tot}}$ of the cell.

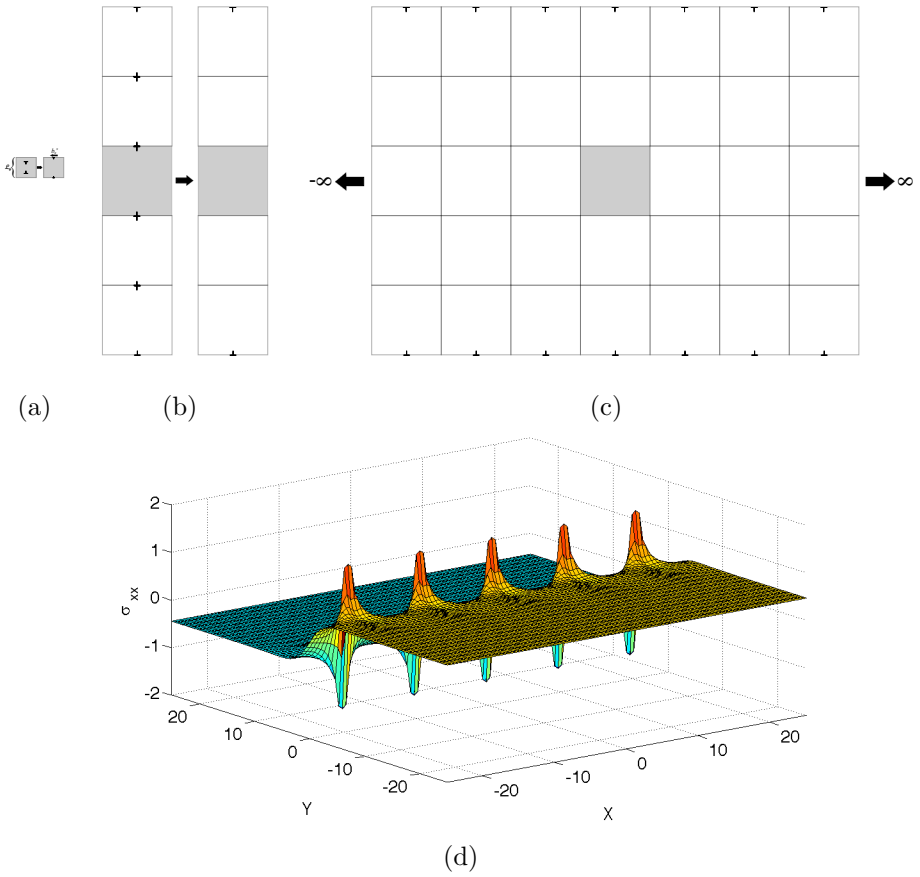


**Figure 3.** (a) Replacing a dislocation configuration with another one having the same dipole moment but with dislocations located at the cell boundary. Such replacement does not change the magnitude of the stress error. (b) When the periodic images along the $y$-axis are superimposed, the dislocations on interior cell boundaries exactly cancel out, leaving only the outermost (oppositely-signed) dislocations. (c) Because PBC is also applied along the $x$-axis (through analytic summation), the remaining configuration is equivalent to two oppositely-signed dislocation arrays that contribute to an overall (spurious) constant stress field in the (shaded) primary cell. (d) Numerical evaluation of the stress field $\sigma_{xx}$ (in arbitrary unit) due to a periodic array of dislocations with Burgers vector $b_x$. The stress field goes to non-zero constants in the limit of $y \to \pm\infty$.

*4.4.2. Constant spurious field* Now let us consider the case of $\mathbf{b}^{\text{tot}} = 0$ again. In general, DD simulations include numerous dislocations in the simulation cell. However, the erroneous stress term **C** will be identical to another simulation cell containing much fewer dislocations as long as their dipole moments are the same, as shown in the previous section. Therefore,

without loss of generality, in order to derive the expression for $\mathbf{C}$, we only need to consider a cell containing a single dislocation dipole, as shown in figure 3(a).

To be specific, let us assume the Burgers vectors of the dislocations to be along the $x$-direction and the two dislocations are separated along the $y$-direction, corresponding to the $x$-$y$ component of the dipole moment tensor $\mathbf{D}$.

Furthermore, we can increase the distance between the two dislocations while reducing the magnitude of their Burgers vectors accordingly without changing the $\mathbf{D}$ tensor. In particular, we would like to put the two dislocations at cell boundaries so that $y$-separation is $\mathcal{L}_y$. If the Burgers vector of the top dislocation is $b_x^{\rm s}$, then the dipole moment is $D_{xy} = b_x^{\rm s}\,\mathcal{L}_y$.

We now consider the case where the stress field is summed analytically in $x$-direction and numerically (with a truncation) in $y$-direction. As shown in figure 3(b), the dislocations from adjacent cells in $y$-direction overlap in location but have opposite Burgers vectors. Therefore, all dislocations cancel each other except those in the two rows at the very top and the very bottom. Therefore, the stress field inside the (primary) cell is a constant, and is the superposition of the contribution from two oppositely signed 1D dislocation arrays located at $y \to \pm\infty$. This constant is precisely the spurious field $\mathbf{C}$ because the internal stress field produced by dislocations averaged over the simulation cell should be zero [20].

By taking the limit of $Y \to -\infty$ in Eq. (9), it can be shown that the stress field from the top dislocation array in the primary cell is $\mu b_x^{\rm s}/[(1-\nu)\mathcal{L}_x]$. The bottom dislocation array makes the same stress contribution, so that the constant stress field inside the primary cell is the following,

$$C_{xx}^{\rm xanl} = \frac{2\,\mu\,b_x^{\rm s}}{(1-\nu)\mathcal{L}_x} = \frac{2\,\mu}{(1-\nu)\mathcal{L}_x\mathcal{L}_y}\,D_{xy} \tag{57}$$

This proves Eq. (48). The long range stress field $C_{xx}$ can be identified with the strain relief caused by misfit dislocations at the interface of heteroepitaxial films.

The same approach can be applied to a screw dislocation dipole with Burgers vector $b_z^{\rm s}$ for the top dislocation. In this case, the constant stress field inside the primary cell is,

$$C_{xz}^{\rm xanl} = \frac{2\,\mu\,b_z^{\rm s}}{2\,\mathcal{L}_x} = \frac{\mu}{\mathcal{L}_x\mathcal{L}_y}\,D_{zy} \tag{58}$$

This proves Eq. (50). That a periodic array of screw dislocations has long range stress field is consistent with the fact that a pure twist boundary (with no long range stress field) must consist of two or more (non-parallel) arrays of screw dislocations. Eqs. (52) and (54) can be proved in a similar way.

*4.4.3. Linear spurious field* When PBC is applied in both directions to a DD simulation cell containing multiple dislocations, the total Burgers vector is usually constrained to be zero. However, in this paper we do not wish to exclude the possibility of a non-zero total Burgers vector in such simulations, as discussed in Section 4.3. Since the coefficient $\mathbf{B}$ is proportional to $\mathbf{b}^{\rm tot}$ and does not depend on other moments of the dislocation distribution, without loss of generality, it is sufficient to consider a single dislocation located at the origin,

in order to derive the expression for $\mathbf{B}$. Such a configuration contains no net dipole moment which may give rise to a non-zero $\mathbf{C}$ term, as derived above. To obtain the coefficient $\mathbf{B}$, we can determine the stress values at two points on the edge of the simulation cell, which should be equal (due to PBC) if $\mathbf{B} = 0$. This is similar to the idea of "ghost" dislocations [20].

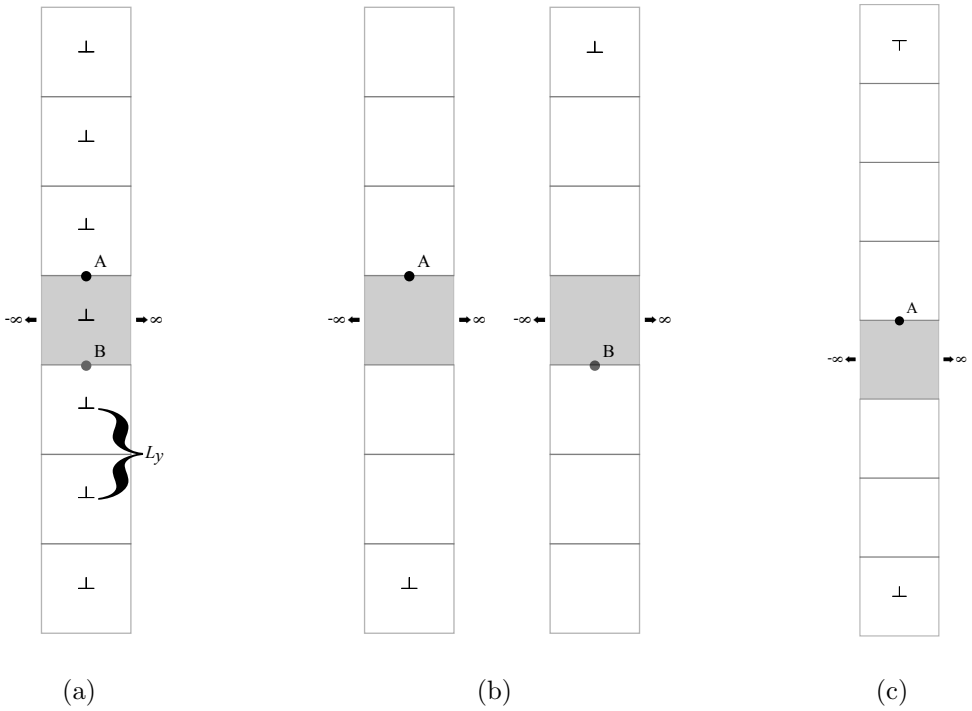


**Figure 4.** Origin of the linear term for stresses calculated using the analytic sum in the $x$-direction and the numerical sum in the $y$-direction. Each dislocation symbol represents a periodic array of dislocations along the $x$-direction. (a) The linear term is evaluated from the difference in stress at the two points **A** and **B**, divided by the distance between them, $\mathcal{L}_y$. (b) Most of the image dislocations cancel when the stresses at **A** and **B** are subtracted, except for one array for each location, as marked here. (c) The difference between the stress field at **A** and **B** is the same as the stress at **A** arising from two oppositely signed dislocation arrays shown here.

As shown in figure 4, we consider the stress values at points $\mathbf{r}^A$ and $\mathbf{r}^B$. The difference between the two stress values, divided by $\mathcal{L}_y$, equals the coefficient $\mathbf{B}$ of the spurious linear term, i.e.

$$\mathbf{B}^{\text{xanl}} = \frac{\boldsymbol{\sigma}(\mathbf{r}^A) - \boldsymbol{\sigma}(\mathbf{r}^B)}{\mathcal{L}_y} \tag{59}$$

At the same time, it can be shown that $\boldsymbol{\sigma}(\mathbf{r}^A) - \boldsymbol{\sigma}(\mathbf{r}^B)$ is exactly the same as the stress field of two end rows of dislocations at point $\mathbf{r}^A$, as shown in figure 4(c). Following the same procedure as in the above derivation of $C_{xx}^{\text{xanl}}$, we find

$$\boldsymbol{\sigma}(\mathbf{r}^A) - \boldsymbol{\sigma}(\mathbf{r}^B) = -\frac{2\,\mu\, b_x^{\text{s}}}{(1-\nu)\mathcal{L}_x} \tag{60}$$

Therefore,

$$B_{xx}^{\text{xanl}} = -\frac{2\,\mu\, b_x^{\text{s}}}{(1-\nu)\mathcal{L}_x\mathcal{L}_y} = -\frac{2\,\mu}{(1-\nu)\mathcal{L}_x\mathcal{L}_y}\, b_x^{\text{tot}} \tag{61}$$

This proves Eq. (47).

The same approach can be applied to a single screw dislocation with Burgers vector $b_z^{\text{s}}$ at the origin. In this case, the coefficient of the linear spurious field is,

$$B_{xz}^{\text{xanl}} = -\frac{2\,\mu\, b_z^{\text{s}}}{2\,\mathcal{L}_x} = -\frac{\mu}{\mathcal{L}_x\mathcal{L}_y}\, b_z^{\text{tot}} \tag{62}$$

This proves Eq. (49). Eqs. (51) and (53) can be proved in a similar way.

## 5. Generalization to Anisotropic Elasticity

In this section, we discuss the solution to the conditional convergence problem in 2D DD simulations based on anisotropic elasticity with singular stress expressions.

### *5.1. Stress Field of Periodic Dislocation Array*

According to the Stroh theory [24], the stress field of an infinitely long straight dislocation line along the $\mathbf{t}$ direction with Burgers vector $\mathbf{b}$ at point $\mathbf{x}$ is the following, assuming the Einstein convention for repeated Roman indices [16],

$$\sigma_{ij}(\mathbf{x}) = \frac{1}{2\pi\,\mathsf{i}}\sum_{\alpha=1}^{6} c_{ijkl}\,(m_l + p_\alpha n_l)\,A_{k\alpha}\,L_{s\alpha}\,b_s\,\frac{\text{Sgn}[\text{Im}(p_\alpha)]}{\mathbf{m}\cdot\mathbf{x} + p_\alpha\mathbf{n}\cdot\mathbf{x}} \tag{63}$$

where $c_{ijkl}$ is the elastic stiffness tensor, and $\mathbf{m}$, $\mathbf{n}$, $\mathbf{t}$ form a right-handed coordinate system. The index $i$ is not to be confused with $\mathsf{i} = \sqrt{-1}$. $p_\alpha$ are the roots of the sextic equation. $\text{Sgn}[\text{Im}(p_\alpha)] = \pm 1$ is the sign of the imaginary part of $p_\alpha$. $\mathbf{A}_\alpha$ and $\mathbf{L}_\alpha$, when combined, form the six-dimensional eigenvector. They satisfy the following relations [25],

$$L_{j\alpha} = -\,n_i\,c_{ijkl}(m_l + p_\alpha n_l)\,A_{k\alpha} \tag{64}$$

$$p_\alpha L_{j\alpha} = m_i\,c_{ijkl}(m_l + p_\alpha n_l)\,A_{k\alpha} \tag{65}$$

For our purpose, $\mathbf{m}$, $\mathbf{n}$ and $\mathbf{t}$ are unit vectors along the $x$, $y$ and $z$ axes, respectively. Hence $m_l = \delta_{1l}$, $n_l = \delta_{2l}$, $\mathbf{m}\cdot\mathbf{x} = x$, and $\mathbf{n}\cdot\mathbf{x} = y$. Making these substitutions,

$$\sigma_{ij}(x,y) = \frac{1}{2\pi\,\mathsf{i}}\sum_{\alpha=1}^{6}(c_{ijk1} + p_\alpha c_{ijk2})\,A_{k\alpha}\,L_{s\alpha}\,b_s\,\frac{\text{Sgn}[\text{Im}(p_\alpha)]}{x + p_\alpha y} \tag{66}$$

The stress of a periodic array of dislocations arranged along the $x$-axis with periodicity $\mathcal{L}_x$ is,

$$\sigma_{ij}^{\text{xPBC}}(x,y) = \frac{1}{2\pi\,\mathsf{i}}\sum_{\alpha=1}^{6}(c_{ijk1} + p_\alpha c_{ijk2})\,A_{k\alpha}\,L_{s\alpha}\,b_s\sum_{m=-\infty}^{\infty}\frac{\text{Sgn}[\text{Im}(p_\alpha)]}{(x - m\mathcal{L}_x) + p_\alpha y} \tag{67}$$

The summation over $m$ can be performed analytically [26] to give

$$\sum_{m=-\infty}^{\infty} \frac{1}{(x - m\mathcal{L}_x) + p_\alpha y} = \frac{\pi}{\mathcal{L}_x} \frac{\cos\left(\frac{\pi}{\mathcal{L}_x}(x + p_\alpha y)\right)}{\sin\left(\frac{\pi}{\mathcal{L}_x}(x + p_\alpha y)\right)} \tag{68}$$

In the limit of $y \to +\infty$, the above expression becomes

$$\lim_{y\to+\infty} \frac{\pi}{\mathcal{L}_x} \frac{\cos\left(\frac{\pi}{\mathcal{L}_x}(x + p_\alpha y)\right)}{\sin\left(\frac{\pi}{\mathcal{L}_x}(x + p_\alpha y)\right)} = -\frac{\pi\,\mathsf{i}}{\mathcal{L}_x}\,\mathrm{Sgn}[\mathrm{Im}(p_\alpha)] \tag{69}$$

This can be shown by expressing $p_\alpha$ as $\mathrm{Re}(p_\alpha) + \mathrm{Im}(p_\alpha)$ and expanding the cos and sin functions with complex arguments into cosh and sinh functions with real arguments. Using Eqs. (67)-(69), and noticing that $(\mathrm{Sgn}[\mathrm{Im}(p_\alpha)])^2 = 1$, we can show that

$$\lim_{y\to+\infty} \sigma_{ij}^{\mathrm{xPBC}}(x, y) = -\frac{b_s}{2\mathcal{L}_x} \sum_{\alpha=1}^{6} (c_{ijk1} + p_\alpha c_{ijk2})\; A_{k\alpha}\, L_{s\alpha} \tag{70}$$

Similarly, the stress of a periodic array of dislocations arranged along the $y$-axis with periodicity $\mathcal{L}_y$ is,

$$\sigma_{ij}^{\mathrm{yPBC}}(x, y) = \frac{1}{2\pi\,\mathsf{i}} \sum_{\alpha=1}^{6} (c_{ijk1} + p_\alpha c_{ijk2})\, A_{k\alpha}\, L_{s\alpha}\, b_s \sum_{n=-\infty}^{\infty} \frac{\mathrm{Sgn}[\mathrm{Im}(p_\alpha)]}{x + p_\alpha(y - n\mathcal{L}_y)} \tag{71}$$

Note that

$$\sum_{n=-\infty}^{\infty} \frac{1}{x + p_\alpha(y - n\mathcal{L}_y)} = \frac{\pi}{p_\alpha\mathcal{L}_y} \frac{\cos\left(\frac{\pi}{p_\alpha\mathcal{L}_y}(x + p_\alpha y)\right)}{\sin\left(\frac{\pi}{p_\alpha\mathcal{L}_y}(x + p_\alpha y)\right)} \tag{72}$$

In the limit of $x \to +\infty$, the above expression becomes

$$\lim_{x\to+\infty} \frac{\pi}{p_\alpha\mathcal{L}_y} \frac{\cos\left(\frac{\pi}{p_\alpha\mathcal{L}_y}(x + p_\alpha y)\right)}{\sin\left(\frac{\pi}{p_\alpha\mathcal{L}_y}(x + p_\alpha y)\right)} = \frac{\pi\,\mathsf{i}}{p_\alpha\mathcal{L}_y}\,\mathrm{Sgn}[\mathrm{Im}(p_\alpha)] \tag{73}$$

Hence,

$$\lim_{x\to+\infty} \sigma_{ij}^{\mathrm{yPBC}}(x, y) = \frac{b_s}{2\mathcal{L}_y} \sum_{\alpha=1}^{6} \left(\frac{c_{ijk1}}{p_\alpha} + c_{ijk2}\right)\; A_{k\alpha}\, L_{s\alpha} \tag{74}$$

### *5.2. Conditional Convergent Terms in 2D Summation*

Earlier, it was proved that the effect of conditional convergence in 2D PBC is to introduce a linear and constant stress field in the simulation cell. This conclusion is independent of whether the elastic medium is isotropic or anisotropic. Therefore, the same procedure applies to 2D DD simulations in anisotropic elastic medium. The Peach-Koehler force due to the spurious stress field needs to be subtracted from every dislocation.

In the case of analytic sum in $x$-direction and numerical sum in $y$-direction, the spurious stress field has the following form,

$$\boldsymbol{\sigma}^{\text{sp}} = \mathbf{B}^{\text{xanl}}\, y + \mathbf{C}^{\text{xanl}} \tag{75}$$

where $\mathbf{B}^{\text{xanl}}$ and $\mathbf{C}^{\text{xanl}}$ are related to the stress field of the infinite dislocation array (periodic along the $x$-axis) in the limit of $y \to \pm\infty$, i.e. Eq. (70). The analytic expressions for the $\mathbf{B}$ and $\mathbf{C}$ tensors are following.

$$B_{ij}^{\text{xanl}} = -\frac{1}{\mathcal{L}_x \mathcal{L}_y} \sum_{\alpha=1}^{6} \left(c_{ijk1} + p_\alpha c_{ijk2}\right)\, A_{k\alpha}\, L_{s\alpha} \cdot \left(\sum_q b_s^{(q)}\right) \tag{76}$$

$$C_{ij}^{\text{xanl}} = \frac{1}{\mathcal{L}_x \mathcal{L}_y} \sum_{\alpha=1}^{6} \left(c_{ijk1} + p_\alpha c_{ijk2}\right)\, A_{k\alpha}\, L_{s\alpha} \cdot \left(\sum_q b_s^{(q)} y^{(q)}\right) \tag{77}$$

Using Eq. (64) and the orthogonality condition [25] $\sum_{\alpha=1}^{6} L_{j\alpha} L_{k\alpha} = 0$, we can show that $n_i\, B_{ij}^{\text{xanl}} = 0$ and $n_i\, C_{ij}^{\text{xanl}} = 0$. In other words, $B_{2j}^{\text{xanl}} = 0$ and $C_{2j}^{\text{xanl}} = 0$. This is sufficient to show that the linear stress field $\mathbf{B}^{\text{xanl}}\, y$ satisfies the equilibrium condition. Eqs. (76) and (77) reduce to Eqs. (47)-(50) in the isotropic elasticity limit. In the case of analytic sum in $y$-direction and numerical sum in $x$-direction, the spurious stress field has the following form,

$$\boldsymbol{\sigma}^{\text{sp}} = \mathbf{B}^{\text{yanl}}\, x + \mathbf{C}^{\text{yanl}} \tag{78}$$

where $\mathbf{B}^{\text{yanl}}$ and $\mathbf{C}$ are related to the stress field of the infinite dislocation array (periodic along $y$-axis) in the limit of $x \to \pm\infty$, i.e. Eq. (74). The analytic expressions for the $\mathbf{B}$ and $\mathbf{C}$ tensors are the following.

$$\mathbf{B}_{ij}^{\text{yanl}} = \frac{1}{\mathcal{L}_x \mathcal{L}_y} \sum_{\alpha=1}^{6} \left(\frac{c_{ijk1}}{p_\alpha} + c_{ijk2}\right)\, A_{k\alpha}\, L_{s\alpha} \cdot \left(\sum_q b_s^{(q)}\right) \tag{79}$$

$$\mathbf{C}_{ij}^{\text{yanl}} = -\frac{1}{\mathcal{L}_x \mathcal{L}_y} \sum_{\alpha=1}^{6} \left(\frac{c_{ijk1}}{p_\alpha} + c_{ijk2}\right)\, A_{k\alpha}\, L_{s\alpha} \cdot \left(\sum_q b_s^{(q)} x^{(q)}\right) \tag{80}$$

Using Eq. (65) and the orthogonality condition [25] $\sum_{\alpha=1}^{6} L_{j\alpha} L_{k\alpha} = 0$, we can show that $m_i\, B_{ij}^{\text{yanl}} = 0$ and $m_i\, C_{ij}^{\text{yanl}} = 0$. In other words, $B_{1j}^{\text{xanl}} = 0$ and $C_{1j}^{\text{yanl}} = 0$. This is sufficient to show that the linear stress field $\mathbf{B}^{\text{yanl}}\, x$ satisfies the equilibrium condition. Eqs. (79) and (80) reduce to Eqs. (51)-(54) in the isotropic elasticity limit.

## 6. Conclusion

The main objective of this paper is to solve the problem of conditional convergence in 2D DD simulations with imposed 2D PBC. This problem arises because the stresses far from a 1D periodic array of dislocations do not necessarily go to zero. The result from the numerical sum needs to be corrected to ensure that spurious stress fields do not corrupt simulation results. Analytic expressions were derived for the linear and constant spurious stress fields,

which, when subtracted, makes the stress summation absolutely convergent. For 2D DD simulations, this solution is more convenient and efficient to use than the "ghost" dipole method [20] developed previously. The solution has been derived for both isotropic and anisotropic elasticity.

## 7. Acknowledgements

We would like to acknowledge helpful conversations with Prof. E. Van der Giessen and his student, A. E. Boerma. We would like to thank Prof. D. M. Barnett for careful reading of our manuscript and for pointing out the proof that the linear correction field satisfies the equilibrium condition in an anisotropic medium. William Kuykendall is supported by a Stanford Graduate Fellowship.

## References

[1] Needleman, A and van der Giessen, E. Discrete dislocation plasticity: a simple planar model. Modelling Simul. Mater. Sci. Eng. **3**, 689-735 (1995).

[2] Amodeo, RJ and Ghoniem, NM. Dislocation dynamics. I. A proposed methodology for deformation micromechanics. Quarterly Journal of Mechanics and Applied Mathematics **41**, 6958-6967 (1990).

[3] Amodeo, RJ and Ghoniem, NM. Dislocation dynamics. II. Applications to the formation of persistent slip bands, planar arrays, and dislocation cells. Quarterly Journal of Mechanics and Applied Mathematics **41**, 6968-6976 (1990).

[4] Chakravarthy, SS and Curtin, WA. New algorithms for discrete dislocation modeling of fracture. Modelling Simul. Mater. Sci. Eng. **19**, 045009 (2011).

[5] Yefimov, S; Groma, I; and van der Giessen, E. A comparison of a statistical-mechanics based plasticity model with discrete dislocation plasticity calculations. J. Mech. Phys. Solids **52**, 279-300 (2004).

[6] Csikor, FF and Groma, I. Probability distribution of internal stress in relaxed dislocation systems. Phys. Rev. B **70**, (2004).

[7] Ispánovity, PD; Groma, I; Hoffelner, W; Samaras, M. Abnormal subgrain growth in a dislocation-based model of recovery. Modelling Simul. Mater. Sci. Eng. **19**, 045008 (2011).

[8] Bakó, B; Groma, I; Gyřgyi, G; Zimányi, G. Dislocation patterning: The role of climb in meso-scale simulations. Comp. Mat. Sci. **38**, 22-28 (2006).

[9] Cleveringa, HHM; van der Giessen, E; Needleman, A. Comparison of discrete dislocation and continuum plasticity predictions for a composite material. Acta Materialia. **45**,8 3163-3179 (1997).

[10] Shu, JY; Fleck, NA; van der Giessen, E; Needleman, A. Boundary layers in constrained plastic flow: comparison of nonlocal and discrete dislocation plasticity. J. Mech. Phys. Solids **49** 1361-1395 (2001).

[11] Gaucherin, G; Hofmann, F; Belnoue, JP; Korsunsky, AM. Crystal plasticity and hardening: a dislocation dynamics study. Mesomechanics 2009, Procedia Engineering **1** 241-244 (2009).

[12] Lefebvre, S; Devincre, B; Hoc, T. Yield stress strengthening in ultrafine-grained metals: A two-dimensional simulation of dislocation dynamics. J. Mech. Phys. Solids **55** 788-802 (2007).

[13] Zeng, XH and Hartmaier, A. Modeling size effects on fracture toughness by dislocation dynamics. Acta Materialia **58** 301-310 (2010).

[14] Razafindrazaka, M; Tanguy, D; Delafosse, D. Defect hardening modeled in 2D discrete dislocation dynamics. Materials Science & Engineering A **527** 150-156 (2009).

[15] Cai, W; Arsenlis, A; Weinberger, CR; Bulatov, VV. A non-singular continuum theory of dislocations. J. Mech. Phys. Solids **54**, 561-587 (2006).

[16] Hirth, JP and Lothe, J. Theory of Dislocations, 2nd ed. (Krieger, Malabar, FL, 1992).

[17] Pang, Linyong. A new O(N) method for modeling and simulating the behavior of a large number of dislocations in anisotropic linear elastic media. PhD Thesis, Stanford University, 2000. Chapter 2.

[18] Rudin, Walter. Principles of Mathematical Analysis, 3rd ed. (McGraw-Hill, New York, 1976.) Chapter 3, pp. 71-72.

[19] Bromwich, T. J. I'A. and MacRobert, T. M. An Introduction to the Theory of Infinite Series, 3rd ed. (Chelsea, New York, 1991). p. 74.

[20] Cai, W; Bulatov, VV; Chang, J; and Li, J. Periodic image effects in dislocation modelling. Philos. Mag. A **83**, 539-567 (2003).

[21] de Leeuw, S. W.; Perram, J. W.; and Smith, E. R. Simulation of Electrostatic Systems in Periodic Boundary Conditions. I. Lattice Sums and Dielectric Constants. Proc. R. Soc. A **393**, 27-56 (1980).

[22] Boerma, A. E. Evaluating the fields of periodic dislocation distributions using the Fourier transform. Bachelors thesis, University of Groningen, 2012.

[23] Boerma, A. E. and van der Giessen, E. private communication.

[24] Stroh, AN. Steady state problems in anisotropic elasticity. J. Math. Phys., **41**, 77-103 (1962).

[25] Bacon, D. J.; Barnett, D. M.; and Scattergood, R. O. Anisotropic continuum theory of lattice defects, Prog. Mater. Sci. **23** 51-262 (1979)

[26] Morse, Philip M. and Feshbach, Herman. Methods of Theoretical Physics, (McGraw-Hill, New York, 1953). Part I, Chapter 4.